

## Structural changes and enhanced accessibility of natural cellulose pretreated by mechanical activation

Huayu Hu · Yanjuan Zhang · Xiaoping Liu ·  
Zuqiang Huang · Yanmeng Chen · Mei Yang ·  
Xingzhen Qin · Zhenfei Feng

Received: 8 May 2013 / Revised: 30 September 2013 / Accepted: 22 October 2013 /  
Published online: 29 October 2013  
© Springer-Verlag Berlin Heidelberg 2013

**Abstract** A kind of natural cellulose, bleached pine pulp (BPP), was pretreated by mechanical activation (MA) using a self-designed stirring ball milling. The effect of MA pretreatment on the dissolving capacity and molecular chain structure of BPP were investigated by the determination of alkaline solubility ( $S_a$ ) and degree of polymerization (DP). In addition, the changes in crystal structure of MA-pretreated BPP with different milling times were qualitatively and quantitatively measured by X-ray diffraction and Fourier transform infrared spectroscopy, and the morphology modification was observed by scanning electron microscopy. It was found that MA significantly increased the  $S_a$  and reduced the DP of BPP, contributing to the destruction of inter- and intramolecular hydrogen bonds and macromolecular chains in cellulose. The stable crystal structure of BPP was also remarkably damaged during MA processing, resulting in the variation of surface morphology, the increase of amorphous region ratio and hydrogen bond energy, and the decrease in crystallinity and crystalline size, which efficiently increased the accessibility of natural cellulose and would have positive effects on subsequent treatments. The crystalline form of natural cellulose was not changed by MA, and no new functional groups generated during milling.

**Keywords** Natural cellulose · Mechanical activation · Pretreatment ·  
Crystal structure · Accessibility · Degree of polymerization

---

H. Hu · Y. Zhang · X. Liu · Z. Huang (✉) · Y. Chen · M. Yang · X. Qin · Z. Feng  
School of Chemistry and Chemical Engineering, Guangxi University, Nanning 530004, China  
e-mail: huangzq@gxu.edu.cn

Y. Zhang  
Guangxi Research Institute of Chemical Industry, Nanning 530001, China

## Introduction

Natural cellulose, the most abundantly available bio-polymer in nature, is a virtually inexhaustible renewable raw material with fascinating properties [1, 2]. Cellulose is already used often in our daily lives and has enormous potential with an expanded role as a source of fuels and commodity chemicals for the future [3]. Cellulose is a hydrophilic and biodegradable linear homopolymer, composed of D-Anhydro glucopyranose units (AGU) linked by  $\beta$ -(1–4) glycosidic bonds. The free hydroxyl functionalities in each AGU form inter- and intramolecular hydrogen bonds readily, and the linear cellulose chains also form an aggregated “fringed fibrillar” supramolecular structure of cellulose [4, 5]. This highly ordered and stable crystal structure of cellulose makes it difficult to dissolve in common solvent and resists assault of the reagents, which restrict its full potential in applications [6, 7]. In order to make the reagents more accessible to cellulose, pretreatment is a necessary step to disrupt the high crystallinity structure and increase the amorphization of cellulose [8].

Recently, many methods have been studied for the pretreatment of cellulose, including biological or fungal methods, physical treatments (e.g., chipping, milling, grinding, and gamma ray irradiation), chemical processes (e.g., acid hydrolysis, alkali hydrolysis, organosolv process), physicochemical processes (e.g., autohydrolysis, steam explosion, ammonia fiber explosion, CO<sub>2</sub> explosion, and hot-compressed water pretreatment) and their combination methods [8–12]. Pretreatment is an important tool for practical cellulose conversion processes because it can break the crystalline structure of cellulose and make the cellulose more accessible to the reagents. Every pretreatment method has its own advantages, but also has some drawbacks. For instance, toxic and inhibitory compounds can be generated in the process of some pretreatments, which hamper the efficiency of the subsequent processing [13]. So, it is necessary to choose a suitable pretreatment technology based on the subsequent processing steps of cellulose.

Nowadays, the development of simple, effective and environmentally friendly methods for the pretreatment of cellulose biomass is being actively pursued. Mechanical activation (MA), usually carried out by high-energy milling, refers to the use of friction, collision, impingement, shear or other mechanical actions to change the crystalline structure and physicochemical properties of solids [14]. The structural disruption, bond rupture and reduction in crystallinity of the solids are induced by intense milling, resulting to the production of activated radicals and functional groups and providing a facile access for reagents to the reactive groups of the solids. In addition, a part of mechanical energy could be converted into internal energy of the milled solids during MA [15]. It is well known that the main disadvantage of MA is high energy requirement [16]. But compared with other methods, MA is considered to be a relatively simple and environmentally friendly procedure attributed to the operations without the use of solvents, intermediate fusion, etc., which can avoid the generation of harmful compounds. Furthermore, with continuous modification and improvement, the MA equipments can be more efficient and lower energy consumption. So, MA is a feasible method for the pretreatment of cellulose biomass, especially for the effective production of high added value products.

In this work, a kind of natural cellulose, bleached pine pulp (BPP), was pretreated by MA using a self-designed stirring ball milling, and the changes in properties of BPP induced by MA pretreatment were systematically investigated. The alkaline solubility ( $S_a$ ) and degree of polymerization (DP) were carried out to determine the influence of MA on the accessibility and molecular chain structure of BPP. In addition, the crystal structure changes of MA-pretreated BPP with different milling times were qualitatively and quantitatively analyzed using X-ray diffraction (XRD) and Fourier transform infrared spectroscopy (FTIR), and surface morphology modification was also investigated by scanning electron microscopy (SEM).

## Experimental

### Materials

Bleached pine pulp, which is the pine lignocellulose treated by pulping and bleaching processes to remove lignin and chromophores, was obtained from a local paper mill (Nanning, China). It had about 87 % cellulose and a DP of 886. This flocculent BPP could easily agglomerate during milling, leading to uneven mechanical force on solids and affect the effect of MA. So, the flocculent BPP was firstly treated by dilute oxalic acid, and then was repeatedly washed with deionized water to neutrality. After vacuum dried at 50 °C, the powdery BPP with better dispersibility was obtained. The powdery BPP with a DP of 237 was used for the following experiments. All reagents were of analytical grade without further purification and obtained from commercial sources, and deionized water was used throughout the work.

### MA pretreatment

Mechanical activation pretreatment of BPP was performed in a self-designed stirring ball mill driven by a commercially available drill press (0.75 kW, maximum drilling diameter = 16 mm) equipped with a speed-tuned motor [17]. For each milling experiment, the BPP sample (10.0 g in each batch) was added into a jacketed stainless steel chamber (1,200 mL) with 300 mL milling balls (6 mm diameter), then the sample was subjected to dry milling at a fixed temperature of 30 °C by circulating the thermostatic water in the jacket of chamber. No other additives were added during MA processing, and the milling was carried out at the speed of 375 rpm for all the batch experiments. The balls were removed after the sample was milled for different designated times (30, 60, 90 and 120 min), then the chamber and milling balls were thoroughly cleaned and dried before the next milling experiment. The resulting samples were stored in a silica-gel desiccator.

### Determination of alkaline solubility

The  $S_a$  of nonactivated and MA-pretreated BPP samples was determined by a modification of the previously reported method [18], and it was carried out as

follows: about 2.0 g (precision 0.1 mg) of the sample was dissolved under magnetic stirring in 98 g of 7 % (wt) NaOH aqueous solution at 30 °C for 1 h. Then the mixed solution was high-speed centrifuged at 3,500 rpm for 30 min. The dissolved part was discarded, and the undissolved part was repeatedly washed with deionized water to neutrality, and then vacuum dried at 50 °C. The  $Sa$  of the BPP samples was calculated from the following equation:

$$Sa = (W - W_U) / W \times 100 \% \quad (1)$$

where  $W$  is the total dry weight of the nonactivated or MA-pretreated BPP sample,  $W_U$  is the dry weight of undissolved BPP sample.

### Determination of DP

The average DP of different BPP samples was measured viscosimetrically in CuEn (copper ethylene diamine solution) using an Ubbelohde viscometer at  $25 \pm 0.1$  °C, and the intrinsic viscosities obtained ( $[\eta]$ ) were converted into the respective values of DP by the following equation [18]:

$$DP^{0.905} = 0.75 [\eta_{CuEn} (\text{cm}^3/\text{g})]. \quad (2)$$

### Surface morphology observation

Surface morphology of the BPP samples was performed using an S-570 SEM (Hitachi, Japan). A thin layer of gold was coated on the samples prior to measurement to prevent charging on the surface. SEM micrographs with different magnifications were obtained to observe the morphologies of different samples.

### XRD analysis

X-ray diffraction analysis was carried out by a Rigaku D/MAX 2500 V diffractometer (Japan) using Cu  $K\alpha$  radiation ( $\lambda = 0.154$  nm) at 40 kV and 30 mA. XRD patterns were recorded by monitoring diffractions from 10° to 40°, with a speed of 0.02°. Crystallinity index (CrI) of the natural cellulose samples was calculated by referring to diffraction intensities of crystalline area and amorphous region according to the following equation [19]:

$$\text{CrI} = \frac{(I_{002} - I_{\text{am}})}{I_{002}} \times 100 \% \quad (3)$$

where  $I_{002}$  is the diffraction intensity of (002) plane and  $I_{\text{am}}$  is the diffraction intensity at  $2\theta = 18^\circ$ .

For estimating the comprising crystalline thickness in sample, the crystalline size of (002) plane,  $D_{002}$ , was calculated based on Scherrer equation [20]:

$$D_{002} = \frac{k\lambda}{\beta \cos\theta} \quad (4)$$

where  $k$  is the Scherrer constant (0.94),  $\lambda$  is wavelength of X-ray tube ( $\lambda = 0.154$  nm),  $\beta$  is FWHM (full width at half maximum) of (002) peak,  $\theta$  is diffraction angle of (002) plane.

### FTIR analysis

Fourier transform infrared spectroscopy analysis was conducted on a Shimadzu 8400S Fourier transform infrared spectrometer (Japan), taking 32 scans for each sample with a resolution of  $4\text{ cm}^{-1}$  in the frequency range of  $4,000\text{--}400\text{ cm}^{-1}$ , and the contribution of  $\text{CO}_2$ , moisture and oxygen in air was eliminated by measuring the background spectra before every sample. The samples for analysis were prepared as follows: the samples (2.0 mg) were mixed with 200.0 mg KBr, respectively, and then the mixtures were pressed into a standard mold to prepare the required discs, which were immediately subjected to FTIR analysis. For the determination of the change in hydrogen bond energy ( $\Delta E$ ) induced by MA,  $\Delta E$  was calculated spectrophotometrically using the following equation [21]:

$$\Delta E = hc(v_2 - v_1) \quad (5)$$

where  $h$  is Plank's constant,  $c$  is the velocity of light,  $v_1$  is the wavenumber of the OH vibration of unmilled BPP sample,  $v_2$  is the wavenumber of the OH vibration of MA-pretreated BPP samples with different milling time.

## Results and discussion

### Effect of milling time on the alkaline solubility of BPP

Natural cellulose without chemical modification and derivatization is difficult to dissolve in common solvents because of its high crystallinity with stiff molecule and numerous inter- and intramolecular hydrogen bonds, and dissolving capacity can be used to evaluate the accessibility of cellulose [22, 23]. Dissolution of cellulose plays an essential role in the production of cellulose derivatives and blended materials, ascribing to that cellulose solution allows homogeneous chemical modifications [24]. NaOH aqueous solution is usually used as a solvent for the dissolution of cellulose because it can lead to an environmentally friendly and simple process. Herein, the solubility of BPP in NaOH aqueous solution was determined to investigate the effect of MA pretreatment on the structure and accessibility of BPP [25]. The influence of milling time on the solubility of BPP in NaOH aqueous solution is presented in Fig. 1, which shows a gradual increase of solubility with milling time. The  $S_a$  of unmilled BPP was only 20 %, but reached to 78 % after mechanically activated for 120 min. During the processing of MA, strong mechanical actions between milling balls destroyed the BPP granules repeatedly, resulting in the destruction of hydrogen bonds and the stable supramolecular structure of natural cellulose, which made BPP more accessible to the reagents and thus increase its dissolving capacity. It also can be observed that the  $S_a$  of BPP approximatively increased linearly as increasing the milling time from 0 to 90 min,

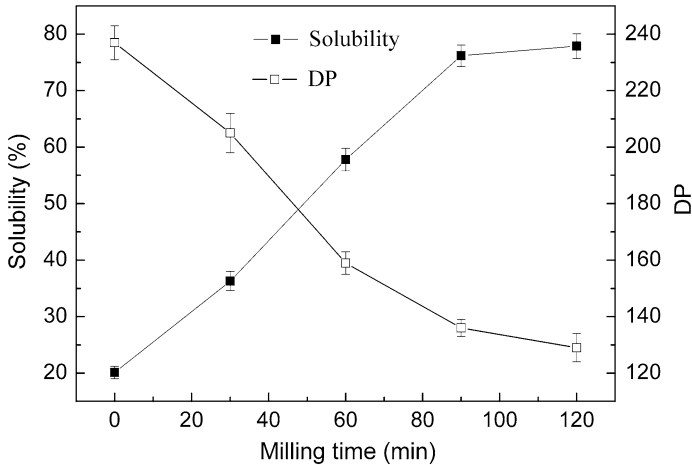


**Fig. 1** Effect of milling time on the *Sa* and DP of BPP. Means of three replicates  $\pm$  standard deviation

but the increasing trend slowed down after 90 min. In the stage of 10 to 90 min, mechanical milling mainly induced the size reduction and structural disorder of cellulose, contributing to the obvious increase of solubility. In the final stage (after 90 min), the agglomeration of fine particles could weaken the direct action of ball milling on cellulose, and the breakage of hydrogen bonds and increase of amorphous phase were not so remarkable, which affected the increment of *Sa* [26]. The detail structure transformations of BPP during milling can be clearly analyzed by the determination of DP, FTIR, XRD, and SEM.

#### Effect of milling time on DP of BPP

Degree of polymerization, a measurement of cellulose chain length, represents the numbers of AGU in cellulose molecules [27]. As shown in Fig. 1, the DP of BPP gradually decreased with increasing the milling time, indicating that ball milling could significantly break the cellulose macromolecular chain and induce the degradation of cellulose. The breakage of the stable and highly ordered structure of cellulose and the generation of short chain cellulose molecules make it more accessible to the reagents and thus increase its dissolving capacity. The decreasing trend of DP of BPP also became slow after milled for 90 min, which is consistent with the increasing trend of *Sa*, revealing that the DP has a direct relation to the dissolving capacity of cellulose in alkaline solution [28].

#### Surface morphology modification

The surface morphologies of different samples can be intuitively observed from SEM micrographs with different magnifications, which are illustrated in Fig. 2. It is found that the surface morphologies of BPP were significantly changed during the processing of MA. As shown in Fig. 2a1 and a2, original BPP consists of flaky or

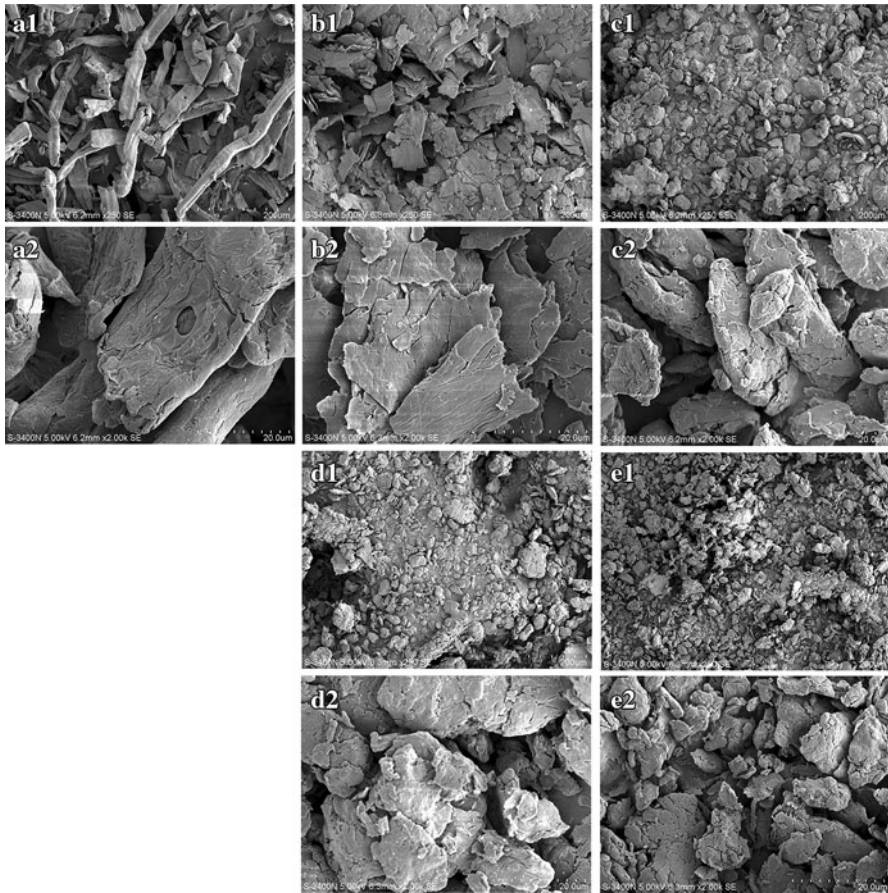


**Fig. 2** SEM micrographs of unmilld BPP (**a1**, **a2**) and MA-pretreated BPP milled for different times with different magnifications: 30 min (**b1**, **b2**), 60 min (**c1**, **c2**), 90 min (**d1**, **d2**), 120 min (**e1**, **e2**)

lathlike fiber bundles with compact surfaces. After MA pretreatment, the BPP particles were greatly destroyed and the fiber bundles were split and fractured, contributing to the generation of small irregular particles with rough and cracky surfaces, and the fibrous structure disappeared gradually. After milled for 120 min, fibrous structure of BPP was completely destroyed, and the particle size of BPP decreased sharply, becoming more uniform. These indicate that the decrease in particle size and ordered structure, increase in specific surface area and amorphization, split and destruction of compact fiber bundles were induced by ball milling, which referred to the use of collision, friction, shear, impingement, or other strong mechanical actions between milling balls to destroy the BPP particles repeatedly. The size reduction and destruction of stable supramolecular structure of cellulose provide a facile access of reagents to the interior of BPP, which can effectively increase its dissolving capacity and help to improve the conditions of subsequent treatments.

## XRD analysis

The XRD patterns of original BPP and MA-pretreated BPP with different milling times are presented in Fig. 3. All the diffraction patterns of the samples show typical spectra of plant cellulose, with the crystalline form of cellulose I [29]. It can be found that the (101) and (10 $\bar{1}$ ) planes have weaker diffraction and overlap with each other, attributing to that BPP contains a certain amount of lignin and hemicellulose, which contribute to the amorphization of natural cellulose. No new diffraction peaks appear in the XRD patterns of MA-pretreated BPP samples, and the location of diffraction peaks does not shift after MA, indicating that MA did not change the crystalline form of natural cellulose. It can be observed clearly that MA pretreatment caused a significant decrease in peak intensity of cellulose and broadening of diffraction peaks, and the (101), (10 $\bar{1}$ ) and (002) planes of activated BPP samples with decreased diffraction gradually overlapped and trended to form a weak and wide diffraction peak. These are attributed to the reduction of crystalline ordered scattering units, resulted from a decrease in crystalline phase, the variation of crystallite size, and the destruction of macromolecular chains and crystalline structure linked with ball impact and collision [30].

To quantitatively analyze the changes in crystal structure of BPP after MA pretreatment, the CrI and  $D_{002}$  were calculated by Eqs. 3 and 4, respectively, and the results are shown in Table 1. It can be seen that the CrI and  $D_{002}$  of MA-pretreated BPP remarkably decreased with an increase in milling time, confirming that ball milling had a notable effect on the deformation of crystal structure and fragmentation of crystalline grains. After MA pretreatment, the initial packing of polymer macromolecules were loosened and changed, which could help to increase the dissolving capacity and reactivity of BPP. In the production of BPP-based materials, the MA-pretreated BPP with more amorphous part and smaller crystalline

**Fig. 3** XRD patterns of unmilled BPP (a), MA-pretreated BPP with different milling times: 30 min (b), 60 min (c), 90 min (d) and 120 min (e)

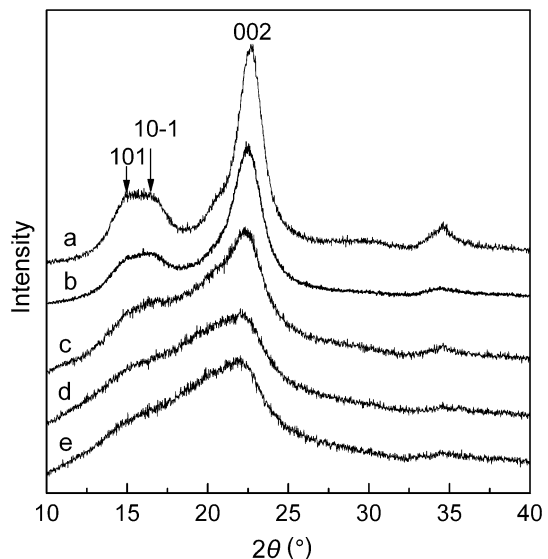




**Table 1** CrI,  $D_{002}$  and Infrared TCI values of unmilled BPP and MA-pretreated BPP with different milling times

Milling time (min)	CrI (%)	$D_{002}$ (nm)	Infrared TCI
0	78.5	4.24	0.483
30	72.7	3.55	0.320
60	43.2	2.88	0.279
90	27.3	1.86	0.221
120	24.1	1.65	0.202

grains can be more active for the subsequent processing, which have obviously favorable influence on the efficient utilization of BPP.

### FTIR analysis

FTIR analysis is a useful tool for obtaining rapid information about the structure of polysaccharides and chemical changes taking place in polysaccharides during various treatments [31]. Figure 4 presents the FTIR spectra of BPP powders before and after MA pretreatment. All the FTIR spectra of the samples show two main absorption regions, presenting at low wavelengths in  $1,800\text{--}700\text{ cm}^{-1}$  and higher wavelengths in  $3,500\text{--}2,700\text{ cm}^{-1}$ , which are consistent with the typical spectra of plant cellulose [29]. The band at  $\sim 897\text{ cm}^{-1}$  assigns to the  $\beta$ -glycosidic linkages between glucose unites in cellulose [32]. The peak at  $\sim 1,590\text{ cm}^{-1}$  is attributed to aromatic skeletal vibrations of lignin [33, 34]. The absorption at  $\sim 1,730\text{ cm}^{-1}$  is due to carbonyl groups of uronic acid from hemicellulose. These can prove that BPP contains not only cellulose, but also other two biopolymers, namely lignin and hemicellulose [35]. Compared with the spectrum of original BPP, it can be observed that no new absorption peaks appear in the spectra of MA-pretreated BPP samples, indicating that no new functional groups generated during MA pretreatment. However, the peak at  $4,000\text{--}2,995\text{ cm}^{-1}$ , related with the hydrogen bonded O–H stretching vibration, shifted to a higher wavenumber as the increase of milling time. This may due to the breakage of inter- and intramolecular hydrogen bonds in main chains of cellulose under the intensive impact of ball milling, increasing the content of free hydroxy groups and then intermolecular hydrogen bonds were reformed by part of these free hydroxy groups [26, 30]. As calculated by Eq. 5, the hydrogen bond energies of the BPP activated for 30, 60, 90 and 120 min were  $4.96 \times 10^{-4}$ ,  $9.93 \times 10^{-4}$ ,  $1.97 \times 10^{-3}$  and  $2.36 \times 10^{-3}$  eV higher than that of nonactivated BPP, respectively. Therefore, it can be seen that MA pretreatment could increase the internal energy of BPP and weaken the stability of hydrogen bond, leading to promote the reactions between reagents and the hydroxyl groups of cellulose.

The infrared Total Crystallinity Index (TCI,  $A_{1,370}/A_{2,900}\text{ cm}^{-1}$ ) of unmilled BPP and MA-pretreated samples with different milling times was determined from the absorption ratios proposed by Nelson and O'Connor [33], and the values are presented in Table 1. The TCI values of MA-pretreated BPP decreased with an increase in milling time, which indicates that the stable crystalline structure of

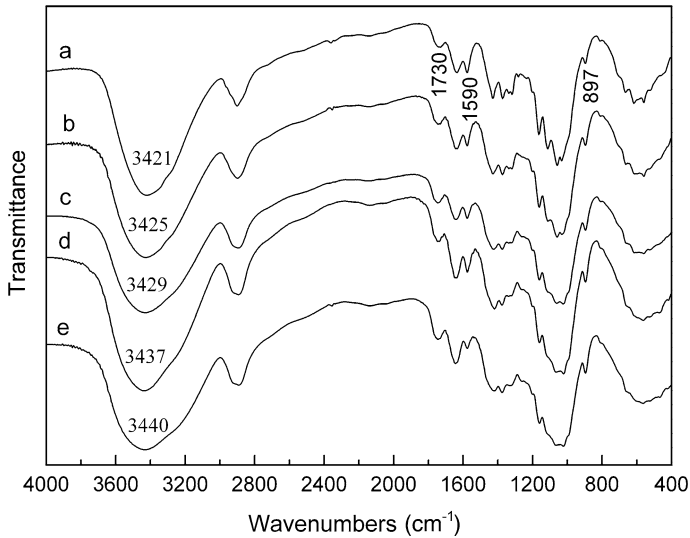


**Fig. 4** FTIR spectra of unground BPP (a), MA-pretreated BPP with different milling times: 30 min (b), 60 min (c), 90 min (d) and 120 min (e)

cellulose had been destroyed by MA, resulting in the presence of less-ordered structure in BPP. The decreasing trend of infrared TCI is consistent with those of CrI and  $D_{002}$ , revealing that the fragmentation of crystalline grains, the deformation of crystalline structure and the increase of amorphization all occurred during the processing of ball milling. As a result, the increase in internal energy, decrease in stability of hydrogen bond and destruction of crystalline structure result in the increase of accessibility of BPP, which would have positive effects on its reactivity and help to enhance the reaction rate and even decrease the dependency on reaction conditions in subsequent processing [30, 36].

## Conclusion

The properties of BPP were significantly changed by MA pretreatment with using a self-designed stirring ball mill. It can be seen that intense milling remarkably broke the macromolecular chain of cellulose and induced the degradation of BPP, contributing to the decrease in DP of BPP with increasing the milling time. SEM observation of different samples showed that the stable and compact structure of BPP was significantly broken by MA, accompanied by particle size reduction and an increase in specific surface area. As shown from the XRD patterns of unground and pretreated BPP samples, MA did not change the crystalline form of natural cellulose, but obviously destroyed the crystal structure of BPP, resulting in the increase of amorphization and the decrease of crystalline size. FTIR analysis indicated that the MA-pretreated BPP had more active hydroxy groups and hydrogen bond energy than the unground sample, and the infrared TCI decreased

with an increase in milling time, resulting from the less-ordered structure in activated BPP samples. These significant changes in molecular chain and crystalline structure properties of BPP induced by MA pretreatment made it more accessible to the reagents, which therefore enhanced its dissolving capacity, and the solubility of BPP obviously increased with the increase of milling time.

Undoubtedly, the destruction in cellulose chain and crystalline structure of BPP, the decrease in stability of hydrogen bond and increase in internal energy and accessibility have positive effects on improving the conditions of subsequent treatments of BPP. So, MA is a simple, efficient and environmentally friendly pretreatment technology, and it is more suitable for application in the production of high added value and high quality natural cellulose-based products. To make MA pretreatment economically feasible for industrial scale-up application, the design, development and improvement of the MA equipments with high efficiency and low energy consumption are required for further research.

**Acknowledgments** This work was supported by National Natural Science Foundation of China (No. 51163002) and Guangxi Natural Science Foundation of China (No. 2013GXNSFBA019028 and No. 2013GXNSFDA019004).

## References

1. Kim J, Yun S (2006) Discovery of cellulose as a smart material. *Macromolecules* 39:4202–4206
2. Guo Y, Wang X, Li D, Du H, Wang X, Sun R (2012) Synthesis and characterization of hydrophobic long-chain fatty acylated cellulose and its self-assembled nanoparticles. *Polym Bull* 69:389–403
3. Ciolacu D, Gorgieva S, Tampu D, Kokol V (2011) Enzymatic hydrolysis of different allomorphic forms of microcrystalline cellulose. *Cellulose* 18:1527–1541
4. Labafzadeh SR, Kavakka JS, Sievänen K, Asikkala J, Kilpeläinen I (2012) Reactive dissolution of cellulose and pulp through acylation in pyridine. *Cellulose* 19:1295–1304
5. Poletto M, Pistor V, Zeni M, Zattera AJ (2011) Crystalline properties and decomposition kinetics of cellulose fibers in wood pulp obtained by two pulping processes. *Polym Degrad Stab* 96:679–685
6. Guo Y, Zhou J, Song Y, Zhang L (2009) An efficient and environmentally friendly method for the synthesis of cellulose carbamate by microwave heating. *Macromol Rapid Commun* 30:1504–1508
7. Zhang Z, Liu B, Zhao ZK (2012) Efficient acid-catalyzed hydrolysis of cellulose in organic electrolyte solutions. *Polym Degrad Stab* 97:573–577
8. Mosier N, Wyman C, Dale B, Elander R, Lee YY, Holtzapfle M, Ladisch M (2005) Features of promising technologies for pretreatment of lignocellulosic biomass. *Bioresour Technol* 96:673–686
9. Alvira P, Tomás-Pejó E, Ballesteros M, Negro MJ (2010) Pretreatment technologies for an efficient bioethanol production process based on enzymatic hydrolysis: a review. *Bioresour Technol* 101:4851–4861
10. Hendriks ATWM, Zeeman G (2009) Pretreatments to enhance the digestibility of lignocellulosic biomass. *Bioresour Technol* 100:10–18
11. Ha SH, Mai NL, An G, Koo Y (2011) Microwave-assisted pretreatment of cellulose in ionic liquid for accelerated enzymatic hydrolysis. *Bioresour Technol* 102:1214–1219
12. Chiaramonti D, Prussi M, Ferrero S, Oriani L, Ottonello P, Torre P, Cherchi F (2012) Review of pretreatment processes for lignocellulosic ethanol production, and development of an innovative method. *Biomass Bioenergy* 46:25–35
13. Kim Y, Ximenes E, Mosier NS, Ladisch MR (2011) Soluble inhibitors/deactivators of cellulase enzymes from lignocellulosic biomass. *Enzyme Microb Technol* 48:408–415
14. Liang X, Huang Z, Zhang Y, Hu H, Liu Z (2013) Synthesis and properties of novel superabsorbent hydrogels with mechanically activated sugarcane bagasse and acrylic acid. *Polym Bull* 70:1781–1794

15. Rossberg M, Khairetdinov EF, Linke E, Boldyrev VV (1982) Effect of mechanical pretreatment on thermal decomposition of silver oxalate under non-isothermal conditions. *J Solid State Chem* 41:266–271
16. Zhu JY, Pan X, Zalesny RS (2010) Pretreatment of woody biomass for biofuel production: energy efficiency, technologies, and recalcitrance. *Appl Microbiol Biotechnol* 87:847–857
17. Huang Z, Xie X, Chen Y, Lu J, Tong Z (2008) Ball-milling treatment effect on physicochemical properties and features for cassava and maize starches. *C R Chimie* 11:73–79
18. Cao Y, Tan H (2002) The properties of enzyme-hydrolyzed cellulose in aqueous sodium hydroxide. *Carbohydr Res* 337:1453–1457
19. Kim S, Holtzaple MT (2006) Effect of structural features on enzyme digestibility of corn stover. *Bioresour Technol* 97:583–591
20. Yu CT, Chen WH, Men LC, Hwang WS (2009) Microscopic structure features changes of rice straw treated by boiled acid solution. *Ind Crops Prod* 29:308–315
21. Dawy M, Shabaka AA, Nada AMA (1998) Molecular structure and dielectric properties of some treated lignins. *Polym Degrad Stab* 62:455–462
22. El Seoud OA, Fidale LC, Ruiz N, D'Almeida MLO, Frollini E (2008) Cellulose swelling by protic solvents: which properties of the biopolymer and the solvent matter. *Cellulose* 15:371–392
23. Le Moigne N, Spinu M, Heinze T, Navard P (2010) Restricted dissolution and derivatization capacities of cellulose fibres under uniaxial elongational stress. *Polymer* 51:447–453
24. Trygg J, Fardim P (2011) Enhancement of cellulose dissolution in water-based solvent via ethanol-hydrochloric acid pretreatment. *Cellulose* 18:987–994
25. Le Moigne N, Navard P (2010) Dissolution mechanisms of wood cellulose fibres in NaOH-water. *Cellulose* 17:31–45
26. Zhang W, Liang M, Lu C (2007) Morphological and structural development of hardwood cellulose during mechanochemical pretreatment in solid state through pan-milling. *Cellulose* 14:447–456
27. Hubbell CA, Ragauskas AJ (2010) Effect of acid-chlorite delignification on cellulose degree of polymerization. *Bioresour Technol* 101:7410–7415
28. Qi H, Chang C, Zhang L (2008) Effects of temperature and molecular weight on dissolution of cellulose in NaOH/urea aqueous solution. *Cellulose* 15:779–787
29. Liao Z, Huang Z, Hu H, Zhang Y, Tan Y (2011) Microscopic structure and properties changes of cassava stillage residue pretreated by mechanical activation. *Bioresour Technol* 102:7953–7958
30. Huang Z, Liang X, Hu H, Gao L, Chen Y, Tong Z (2009) Influence of mechanical activation on the graft copolymerization of sugarcane bagasse and acrylic acid. *Polym Degrad Stab* 94:1737–1745
31. Sun RC, Tomkinson J, Wang YX, Xiao B (2000) Physico-chemical and structural characterization of hemicelluloses from wheat straw by alkaline peroxide extraction. *Polymer* 41:2647–2656
32. Oh SY, Yoo DI, Shin Y, Kim HC, Kim HY, Chung YS, Park WH, Youk JH (2005) Crystalline structure analysis of cellulose treated with sodium hydroxide and carbon dioxide by means of X-ray diffraction and FTIR spectroscopy. *Carbohydr Res* 340:2376–2391
33. Colom X, Carrillo F, Nogués F, Garriga P (2003) Structural analysis of photo degraded wood by means of FTIR spectroscopy. *Polym Degrad Stab* 80:543–549
34. Schwanninger M, Rodrigues JC, Pereira H, Hinterstoisser B (2004) Effects of short-time vibratory ball milling on the shape of FT-IR spectra of wood and cellulose. *Vib Spectrosc* 36:23–40
35. Adel AM, Wahab ZHAE, Ibrahim AA, Shemy MTA (2010) Characterization of microcrystalline cellulose prepared from lignocellulosic materials. Part I. Acid catalyzed hydrolysis. *Bioresour Technol* 101:4446–4455
36. Huang Z, Wang N, Zhang Y, Hu H, Luo Y (2012) Effect of mechanical activation pretreatment on the properties of sugarcane bagasse/poly(vinyl chloride) composites. *Compos Part A* 43:114–120